

Analytical Solutions for Buckling Behavior of Two Directional Functionally Graded Beams Using a Third Order Shear Deformable Beam Theory

*Armağan Karamanlı(0000-0003-3990-6515)

Department of Mechatronics Engineering, Faculty of Engineering and Architecture, Assistant Professor, Istanbul Gelişim University, Istanbul, Turkey.

Received Date: 24.11.2017 Accepted Date: 31.05.2018

Abstract

This paper is dedicated to present a Ritz-type analytical solution for buckling behavior of two directional functionally graded beams (2D-FGBs) subjected to various sets of boundary conditions by employing a third order shear deformation theory. The material properties of the beam vary in both axial and thickness directions according to the power-law distribution. The axial, transverse deflections and rotation of the cross sections are expressed in polynomial forms to obtain the buckling load. The auxiliary functions are added to displacement functions to satisfy the boundary conditions. Simply supported – Simply supported (SS), Clamped-Simply supported (CS), Clamped – clamped (CC) and Clamped-free (CF) boundary conditions are considered. Computed results are compared with earlier works for the verification and convergence studies. The effects of the different gradient indexes, various aspect ratios and boundary conditions on the buckling responses of the two directional functionally graded beams are investigated.

Keywords: Two Directional Functionally Graded Beam, Buckling Behavior, Third Order Shear Deformation Theory, Ritz Method

1. INTRODUCTION

With the advance of the production technology, the functionally graded materials (FGMs) which can be classified as advanced materials formed of two or more different materials whose volume fractions vary continuously in a required direction have been developed to satisfy the new demands of military, aerospace, nuclear energy, biomedical, automotive, marine and civil engineering applications. It has received great attention from researchers due to its lower transverse shear stresses, high resistance to temperature shocks and no interface problems through the layer interfaces [1-22]. In some engineering applications, the FGMs with material properties only varying in one direction are not efficient to fulfill the technical requirements such as the temperature and stress distributions in two or three directions for aerospace craft and shuttles [23].

To obtain more effective high-temperature resistant materials, a new type FGM with material properties varying in two or three directions is needed. However, the number of the studies related to the mechanical and thermal behavior of two-directional

FG structures is still very limited. Based on the the Element Free Galerkin Method, 2D steady-state free and forced vibrations of two-directional functionally graded beams (FGBs) are investigated in [24]. Bending and thermal deformations of FGBs with various end conditions are obtained by employing the state-space based differential quadrature method [25]. The static and free vibration analysis of two-directional FGBs is investigated in [26] by obtaining a symplectic elasticity solution. The fully coupled thermo-mechanical behavior of bi-directional FGM beam structures is studied using an isogeometric finite element model in [27]. Free and forced vibration of Timoshenko two directional functionally graded beams under a moving load is investigated in [28] for the case that the material properties of the 2D-FGB vary exponentially through the length and height directions. Based on the power-law distribution of the material properties, the buckling of Timoshenko beams composed of two directional FGM is studied in [29]. The static behavior of the two directional FGBs by using various beam theories is presented in [30]. An analytical solution for the static deformations of the bi-directional

*Corresponding Author: Armağan Karamanlı, Istanbul Gelişim University, 34215, Istanbul, Turkey, Tel: +90 212 422 7020, armagan_k@yahoo.com

Doi: 10.21541/apjes.357539

functionally graded thick circular beams is developed based on a new shear deformation theory with a logarithmic function in the postulated expression for the circumferential displacement in [31]. The flexure behavior of the two directional FG sandwich beams by using a quasi-3D theory and a meshless method is studied in [32]. The bending and buckling analysis of two-directional functionally graded plates are investigated by employing a new third order shear deformation theory via finite element method [33]. By employing a third order shear deformation theory and exponential material distribution, the free vibration behavior of the 2D-FGBs is investigated in [34].

As it is seen from above discussions, one may easily notice that the most of the studies are related to the static, dynamic and buckling analysis of conventional functionally graded (1D-FG) beams and the number of studies regarding to 2D-FGBs is very limited. According to the best of author's knowledge, there is no reported work on the buckling analysis of the two directional FGBs based on a third order shear deformable beam theory. Shear deformation may have a significant effect on the buckling loads of the thick two directional FGBs, so that a third order shear

deformation theory should be considered for this problem. This paper focuses on the bifurcation buckling of 2D-FGBs based on the power-law variation of material properties with various end conditions, aspect ratios and gradient indexes.

2. THEORY AND FORMULATION

2.1 Homogenization of Material Properties

Consider a two-directional functionally graded beam as shown in Fig. 1 with length L, width b and thickness h. The beam is made of two different constituents. The material properties vary both in the x (along the length of the beam) and z (thickness direction) directions. The origin of the coordinate system is at the midpoint of the beam. In this study, the rule of mixture is used to find the effective material properties at a point. The effective material properties of the beam, Young's modulus E and shear modulus G can be given by

$$E(x, z) = E_1V_1(x, z) + E_2V_2(x, z)$$

$$G(x, z) = G_1V_1(x, z) + G_2V_2(x, z) \quad (1)$$

where E_1, E_2, G_1 and G_2 are the material properties of two constituents, V_1 and V_2 are volume fractions of the constituents. The relation of the volume fractions can be expressed as follows;

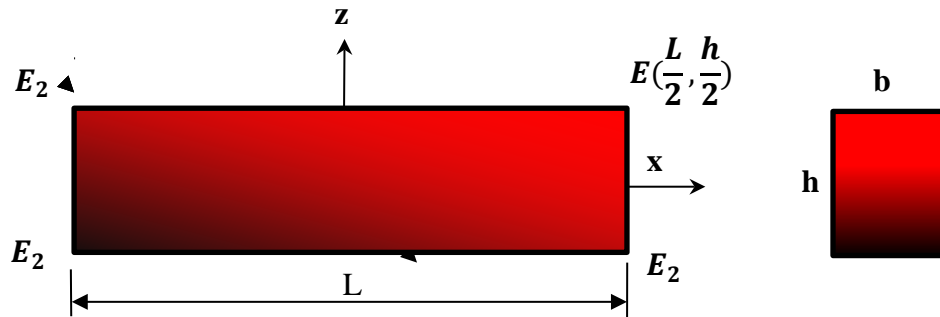


Figure 1. Geometry and coordinate of a two-directional FGB

$$V_1(x, z) + V_2(x, z) = 1 \quad (2)$$

According to the power law variation, the volume fraction of the constitute 1 can be given by

$$V_1(x, z) = \left(\frac{1}{2} + \frac{x}{L}\right)^{p_x} \left(\frac{1}{2} + \frac{z}{h}\right)^{p_z} \quad (3)$$

where p_x and p_z are the gradient indexes which determine the material properties through the thickness (h) and length of the beam (L), respectively. When the p_x and p_z are set to zero then the beam becomes homogeneous. The effective material properties can be found by using the Eqs. (1), (2) and (3) as follows [29],

$$E(x, z) = (E_1 - E_2) \left(\frac{1}{2} + \frac{x}{L}\right)^{p_x} \left(\frac{1}{2} + \frac{z}{h}\right)^{p_z} + E_2$$

$$G(x, z) = (G_1 - G_2) \left(\frac{1}{2} + \frac{x}{L}\right)^{p_x} \left(\frac{1}{2} + \frac{z}{h}\right)^{p_z} + G_2 \quad (4)$$

2.2 Third Order Shear Deformable Beam Theory

The following displacement field is given for the third order shear deformation theory (Reddy Beam Theory (RBT)) [5]

$$U(x, z) = u(x) + z\phi(x) - \alpha z^3 \left(\phi(x) + \frac{dw(x)}{dx}\right)$$

$$W(x, z) = w(x) \quad (5)$$

Here u and w are the axial and transverse displacements of any point on the neutral axis, ϕ the rotation of the cross sections, $\alpha = 4/(3h^2)$. By

using the Eq. (5), the strain-displacement relations

$$\begin{aligned} \epsilon_{xx} &= \frac{\partial U}{\partial x} = \frac{du}{dx} + z \frac{d\phi}{dx} - \alpha z^3 \left(\frac{d\phi}{dx} + \frac{d^2w}{dx^2} \right) \\ \gamma_{xz} &= \frac{\partial U}{\partial z} + \frac{\partial W}{\partial x} = \phi + \frac{dw}{dx} - \beta z^2 \left(\phi + \frac{dw}{dx} \right) \end{aligned} \quad (6)$$

where $\beta = 3\alpha = 4/(h^2)$.

The stress-strain relationship of a two directional functionally graded beam in the material coordinate axes is given by

$$\begin{Bmatrix} \sigma_{xx} \\ \sigma_{xz} \end{Bmatrix} = \begin{bmatrix} E(x, z) & 0 \\ 0 & G(x, z) \end{bmatrix} \begin{Bmatrix} \epsilon_{xx} \\ \gamma_{xz} \end{Bmatrix} \quad (7)$$

where $(\sigma_{xx}, \sigma_{xz})$ are the stresses and $(\epsilon_{xx}, \gamma_{xz})$ are the strains with respect to the axes.

of the RBT are given by

2.3 Variational Formulation of Buckling of Two-Directional Functionally Graded Beam

The strain energy of the beam including the energy associated with the shearing strain can be written as

$$U = \frac{1}{2} \int_V (\sigma_{xx}\epsilon_{xx} + \sigma_{xz}\gamma_{xz}) dV \quad (8)$$

where V is the volume of the beam. By substituting Eqs. (6) and (7) into Eq. (8), the strain energy can be obtained as the form of

$$\begin{aligned} U &= \frac{1}{2} \int_V [E(x, z) \left\{ \left(\frac{du}{dx} \right)^2 + (z^2 + \alpha^2 z^6 - 2\alpha z^4) \left(\frac{d\phi}{dx} \right)^2 + \alpha^2 z^6 \left(\frac{d^2w}{dx^2} \right)^2 \right. \\ &\quad \left. + 2(z - \alpha z^3) \frac{du}{dx} \frac{d\phi}{dx} - 2\alpha z^3 \frac{\partial u}{\partial x} \frac{d^2w}{dx^2} + 2(\alpha^2 z^6 - \alpha z^4) \frac{d\phi}{dx} \frac{d^2w}{dx^2} \right\} + \\ &\quad G(x, z) \left\{ (1 + \beta^2 z^4 - 2\beta z^2) \phi^2 + (1 + \beta^2 z^4 - 2\beta z^2) \left(\frac{dw}{dx} \right)^2 \right. \\ &\quad \left. + 2(1 + \beta^2 z^4 - 2\beta z^2) \phi \frac{dw}{dx} \right\}] dV \end{aligned} \quad (9)$$

The stiffness coefficients can be introduced as follows

$$(A, B, D, C, F, H) = b \int_{-h/2}^{+h/2} (E_1 - E_2) \left(\frac{1}{2} + \frac{z}{h} \right)^{p_z} (1, z, z^2, z^3, z^4, z^6) dz \quad (10)$$

$$(A_s, D_s, F_s) = b \int_{-h/2}^{+h/2} (G_1 - G_2) \left(\frac{1}{2} + \frac{z}{h} \right)^{p_z} (1, z^2, z^4) dz \quad (11)$$

$$(A_1, D_1, F_1, H_1) = b \int_{-h/2}^{+h/2} E_2 (1, z^2, z^4, z^6) dz \quad (12)$$

$$(A_{s1}, D_{s1}, F_{s1}) = b \int_{-h/2}^{+h/2} G_2 (1, z^2, z^4) dz \quad (13)$$

Using Eqs. (4), (10), (11), (12) and (13), the strain energy can be rewritten as

$$\begin{aligned} U &= \frac{1}{2} \int_{-L/2}^{L/2} \left[\left\{ A \left(\frac{1}{2} + \frac{x}{L} \right)^{p_x} + A_1 \right\} \left(\frac{du}{dx} \right)^2 \right. \\ &\quad \left. + \left\{ D \left(\frac{1}{2} + \frac{x}{L} \right)^{p_x} + D_1 \right\} + \alpha^2 \left\{ H \left(\frac{1}{2} + \frac{x}{L} \right)^{p_x} + H_1 \right\} - 2\alpha \left\{ F \left(\frac{1}{2} + \frac{x}{L} \right)^{p_x} + F_1 \right\} \right] \left(\frac{d\phi}{dx} \right)^2 \\ &\quad + \alpha^2 \left\{ H \left(\frac{1}{2} + \frac{x}{L} \right)^{p_x} + H_1 \right\} \left(\frac{d^2w}{dx^2} \right)^2 \\ &\quad + 2 \left(B \left(\frac{1}{2} + \frac{x}{L} \right)^{p_x} - \alpha C \left(\frac{1}{2} + \frac{x}{L} \right)^{p_x} \right) \frac{du}{dx} \frac{d\phi}{dx} - 2\alpha C \left(\frac{1}{2} + \frac{x}{L} \right)^{p_x} \frac{du}{dx} \frac{d^2w}{dx^2} \\ &\quad + 2 \left(\alpha^2 \left\{ H \left(\frac{1}{2} + \frac{x}{L} \right)^{p_x} + H_1 \right\} - \alpha \left\{ F \left(\frac{1}{2} + \frac{x}{L} \right)^{p_x} + F_1 \right\} \right) \frac{d\phi}{dx} \frac{d^2w}{dx^2} \\ &\quad + \left\{ A_s \left(\frac{1}{2} + \frac{x}{L} \right)^{p_x} + A_{s1} \right\} + \beta^2 \left\{ F_s \left(\frac{1}{2} + \frac{x}{L} \right)^{p_x} + F_{s1} \right\} - 2\beta \left\{ D_s \left(\frac{1}{2} + \frac{x}{L} \right)^{p_x} + D_{s1} \right\} \left(\phi^2 + \left(\frac{dw}{dx} \right)^2 \right. \\ &\quad \left. + 2\phi \frac{dw}{dx} \right) dx \end{aligned} \quad (14)$$

The total potential energy of the external axial load (N_0) can be given by

$$V = -\frac{1}{2} \int_{-L/2}^{L/2} N_0 \left(\frac{dw}{dx} \right)^2 dx \quad (15)$$

Using Eqs. 14 and 15, the total potential energy (Π) can be obtained by:

$$\Pi = U + V \quad (16)$$

$$u(x) = \sum_{j=1}^m A_j \theta_j(x), \quad \theta_j(x) = \left(x + \frac{L}{2}\right)^{p_u} \left(x - \frac{L}{2}\right)^{q_u} x^{m-1} \quad (17a)$$

$$w(x) = \sum_{j=1}^m B_j \varphi_j(x), \quad \varphi_j(x) = \left(x + \frac{L}{2}\right)^{p_w} \left(x - \frac{L}{2}\right)^{q_w} x^{m-1} \quad (17b)$$

$$\phi(x) = \sum_{j=1}^m C_j \psi_j(x), \quad \psi_j(x) = \left(x + \frac{L}{2}\right)^{p_\phi} \left(x - \frac{L}{2}\right)^{q_\phi} x^{m-1} \quad (17c)$$

where A_j , B_j and C_j are unknown coefficients to be determined, $\theta_j(x)$, $\varphi_j(x)$ and $\psi_j(x)$ are the shape functions which are proposed for the boundary conditions (BC) to be studied within this paper and

Therefore, the displacement functions $u(x)$, $w(x)$ and the rotation function $\phi(x)$ are presented by the following polynomial series which are satisfy the kinematic boundary conditions given in Table 1.

p_ξ and q_ξ ($\xi = u, w, \phi$) are the boundary exponents of auxiliary functions related with the boundary conditions given in Table 2.

Table 1. Kinematic boundary conditions used for the numerical computations.

BC	$x = -L/2$	$x = L/2$
SS	$u = 0, w = 0$	$w = 0$
CS	$u = 0, w = 0, \phi = 0, w' = 0$	$w = 0$
CC	$u = 0, w = 0, \phi = 0, w' = 0$	$u = 0, w = 0, \phi = 0, w' = 0$
CF	$u = 0, w = 0, \phi = 0, w' = 0$	

Table 2. Boundary exponents for various boundary conditions.

BC	Left end			Right end		
	p_u	p_w	p_ϕ	q_u	q_w	q_ϕ
SS	1	1	0	0	1	0
CS	1	2	1	0	1	0
CC	1	2	1	1	2	1
CF	1	2	1	0	0	0

Substituting Eq. (17) into Eq. (16) and then using principle of minimum potential energy given by Eq. (18), the system of equations given in Eq. (19) is

$$\frac{\partial \Pi}{\partial A_j} = 0, \quad \frac{\partial \Pi}{\partial B_j} = 0, \quad \frac{\partial \Pi}{\partial C_j} = 0 \quad j = 1, 2, 3, \dots, m \quad (18)$$

$$\left(\begin{bmatrix} [K_{11}] & [K_{12}] & [K_{13}] \\ [K_{12}]^T & [K_{22}] & [K_{23}] \\ [K_{13}]^T & [K_{23}]^T & [K_{33}] \end{bmatrix} - N_{cr} \begin{bmatrix} [0] & [0] & [0] \\ [0] & [K_{N_0}] & [0] \\ [0] & [0] & [0] \end{bmatrix} \right) \begin{Bmatrix} \{A\} \\ \{B\} \\ \{C\} \end{Bmatrix} = \begin{Bmatrix} \{0\} \\ \{0\} \\ \{0\} \end{Bmatrix} \quad (19)$$

where $[K_{kl}]$ are the stiffness matrices and $[K_{N_0}]$ is the geometric stiffness matrix. All the matrices are

obtained to calculate the critical buckling loads of two directional FGBs:

symmetric in size $m \times m$. The components of the stiffness matrices are given by:

$$K_{11}(i, j) = \int_{-L/2}^{L/2} \left[A \left(\frac{1}{2} + \frac{x}{L} \right)^{p_x} + A_1 \right] \theta_{i,x} \theta_{j,x} dx,$$

$$K_{12}(i, j) = -\alpha \int_{-L/2}^{L/2} \left[C \left(\frac{1}{2} + \frac{x}{L} \right)^{p_x} \right] \theta_{i,x} \varphi_{j,xx} dx$$

$$K_{13}(i, j) = \int_{-L/2}^{L/2} \left[B \left(\frac{1}{2} + \frac{x}{L} \right)^{p_x} - \alpha C \left(\frac{1}{2} + \frac{x}{L} \right)^{p_x} \right] \theta_{i,x} \psi_{j,x} dx$$

$$\begin{aligned}
K_{22}(i, j) &= \alpha^2 \int_{-L/2}^{L/2} \left[H \left(\frac{1}{2} + \frac{x}{L} \right)^{p_x} + H_1 \right] \varphi_{i,xx} \varphi_{j,xx} dx \\
&\quad + \int_{-L/2}^{L/2} \left[\left\{ A_s \left(\frac{1}{2} + \frac{x}{L} \right)^{p_x} + A_{s1} \right\} + \beta^2 \left\{ F_s \left(\frac{1}{2} + \frac{x}{L} \right)^{p_x} + F_{s1} \right\} \right. \\
&\quad \left. - 2\beta \left\{ D_s \left(\frac{1}{2} + \frac{x}{L} \right)^{p_x} + D_{s1} \right\} \right] \varphi_{i,x} \varphi_{j,x} dx \\
K_{23}(i, j) &= \int_{-L/2}^{L/2} \left[\alpha^2 \left\{ H \left(\frac{1}{2} + \frac{x}{L} \right)^{p_x} + H_1 \right\} - \alpha \left\{ F \left(\frac{1}{2} + \frac{x}{L} \right)^{p_x} + F_1 \right\} \right] \varphi_{i,xx} \psi_{j,x} dx \\
&\quad + \int_{-L/2}^{L/2} \left[\left\{ A_s \left(\frac{1}{2} + \frac{x}{L} \right)^{p_x} + A_{s1} \right\} + \beta^2 \left\{ F_s \left(\frac{1}{2} + \frac{x}{L} \right)^{p_x} + F_{s1} \right\} \right. \\
&\quad \left. - 2\beta \left\{ D_s \left(\frac{1}{2} + \frac{x}{L} \right)^{p_x} + D_{s1} \right\} \right] \varphi_{i,x} \psi_{j,x} dx \\
K_{33}(i, j) &= \int_{-L/2}^{L/2} \left[\left\{ D \left(\frac{1}{2} + \frac{x}{L} \right)^{p_x} + D_1 \right\} + \alpha^2 \left\{ H \left(\frac{1}{2} + \frac{x}{L} \right)^{p_x} + H_1 \right\} - 2\alpha \left\{ F \left(\frac{1}{2} + \frac{x}{L} \right)^{p_x} + F_1 \right\} \right] \psi_{i,x} \psi_{j,x} dx \\
&\quad + \int_{-L/2}^{L/2} \left[\left\{ A_s \left(\frac{1}{2} + \frac{x}{L} \right)^{p_x} + A_{s1} \right\} + \beta^2 \left\{ F_s \left(\frac{1}{2} + \frac{x}{L} \right)^{p_x} + F_{s1} \right\} \right. \\
&\quad \left. - 2\beta \left\{ D_s \left(\frac{1}{2} + \frac{x}{L} \right)^{p_x} + D_{s1} \right\} \right] \psi_{i,x} \psi_{j,x} dx \\
K_{N_0}(i, j) &= \int_{-L/2}^{L/2} \varphi_{i,x} \varphi_{j,x} dx \quad i, j = 1, 2, 3, \dots, m \quad (20)
\end{aligned}$$

3. NUMERICAL RESULTS

In this section, a number of numerical examples are studied to verify the accuracy of the present method and understand the effects of gradient indexes (or material composition), aspect ratios (L/h) and boundary conditions on the buckling behavior of the two directional FGBs. The material properties of the two constitutes are given as follows

Ceramic (Al_2O_3) : $E_1 = 380GPa$ and $\nu_1 = 0.3$

Metal (Aluminium) : $E_2 = 70GPa$ and $\nu_2 = 0.3$

The height of the beam is varied to examine the effect of the shear deformation. Four different boundary conditions, namely simply supported-simply supported (SS), clamped-simply supported (CS), clamped-clamped (CC) and clamped-free (CF) are considered. The following dimensionless buckling load (\bar{N}_{cr}) parameter is used for the representation of the results;

$$\bar{N}_{cr} = \frac{12N_{cr}L^2}{E_2bh^3} \quad (16)$$

To perform the convergence and verification studies, a homogeneous beam is considered and the displacement functions with different number of terms ($m=2, 4, 6, 8, 10$ and 12) are employed. The computed results are presented in terms of dimensionless critical buckling load (\bar{N}_{cr}) considering various gradient indexes in both

directions, aspect ratios and boundary conditions, namely SS, CC and CF. The results from the previous studies [22-23] in terms of dimensionless critical buckling load (\bar{N}_{cr}) are used for comparison purposes in Table 3. It can be seen that the solutions converge quickly for the buckling behavior of SS and CF beams, when the number of terms in the displacement function is set to 6. However, the agreed results are obtained for CC boundary condition by employing 8 terms in the displacement function as given in Table 3. For the sake of accuracy, 8 terms in the polynomial expansion is employed for the extensive buckling analysis of two directional FGBs. In Tables 4-7, the first three dimensionless critical buckling loads of the 2D-FGBs with SS, CS, CC and CF boundary conditions are presented for two different aspect ratios ($L/h=5$ and $L/h=20$) and various gradient indexes in both directions (p_z and p_x). It is seen that that the first three critical buckling loads decrease for all type of end conditions while the gradient indexes increase. It is found that the shear deformation effect becomes very important when the buckling mode number increases. For CC beams, the relative difference between critical buckling loads with respect to variation of the aspect ratio increases as the order of buckling mode becomes higher.

Table 3. Verification and convergence studies, dimensionless critical buckling load (\bar{N}_{cr}) of homogeneous beams with respect to various boundary conditions and aspect ratio change.

L/h	Theory	Boundary Condition			
		SS	CC	CF	
5	HBT [23]	48.5964	152.1588	13.0595	
	HBT [22]	48.5959	152.1470	13.0594	
	Present	2 terms	57.9246	158.9359	13.1552
		4 terms	48.6204	152.2107	13.0595
		6 terms	48.5959	152.1474	13.0594
		8 terms	48.5959	152.1473	13.0594
		10 terms	48.5959	152.1473	13.0594
		12 terms	48.5959	152.1473	13.0594
20	HBT [23]	53.2364	208.9515	13.3730	
	HBT [22]	53.2364	208.9510	13.3730	
	Present	2 terms	64.6387	221.9429	13.4734
		4 terms	53.2658	209.0705	13.3730
		6 terms	53.2364	208.9514	13.3730
		8 terms	53.2364	208.9512	13.3730
		10 terms	53.2364	208.9512	13.3730
		12 terms	53.2364	208.9512	13.3730

Table 4. The first three dimensionless critical buckling load (\bar{N}_{cr}) of SS two directional FGBs with respect to gradient index and aspect ratio change.

\bar{N}_{cr} P_x	L/h=5						L/h=20						
	P_z						P_z						
	0	0.5	1	2	5	10	0	0.5	1	2	5	10	
\bar{N}_{cr1}	0	48.5959	31.8663	24.5838	19.0709	15.6435	14.0512	53.2364	34.5371	26.5619	20.7185	17.4842	15.9099
	0.5	34.2653	23.9967	19.5806	16.2410	13.9967	12.7543	38.5489	26.5203	21.5095	17.8780	15.6754	14.3508
	1	24.9833	18.9430	16.3126	14.2731	12.7414	11.7752	28.5105	21.1149	18.0342	15.7645	14.2169	13.1630
	2	16.6297	14.0784	12.9394	12.0082	11.1712	10.5796	18.6436	15.5435	14.2161	13.1927	12.3578	11.7209
	5	10.9883	10.4117	10.1423	9.8965	9.6200	9.4231	11.9306	11.2801	10.9954	10.7638	10.5342	10.3457
	10	9.5838	9.4222	9.3403	9.2547	9.1464	9.0782	10.3501	10.1862	10.1155	10.0568	9.9942	9.9433
\bar{N}_{cr2}	0	152.1493	102.2720	79.4847	60.8792	46.8874	40.9887	208.9577	135.8733	104.5668	81.4675	68.3289	61.9991
	0.5	98.3238	72.4673	60.2699	49.9335	41.4684	37.4265	145.4236	101.3452	82.7911	69.1136	60.4987	55.4274
	1	70.6470	56.7623	49.8046	43.5674	37.9818	35.0484	107.4457	80.9614	69.5536	60.8733	54.8590	50.9938
	2	51.1536	44.3218	40.8064	37.5317	34.3634	32.5399	75.6765	62.7569	56.9329	52.3287	48.8383	46.3995
	5	36.7035	34.4736	33.3248	32.1987	30.9065	30.0527	52.1439	47.9959	46.0785	44.5051	43.0823	41.9557
	10	31.7045	30.8554	30.4042	29.9131	29.2566	28.8346	43.5041	42.0383	41.3835	40.8346	40.2631	39.7990
\bar{N}_{cr3}	0	252.0228	173.5161	135.8839	102.7968	74.7279	63.8413	456.0778	297.6470	229.3072	178.3198	148.1174	133.7981
	0.5	150.3363	116.1683	98.5777	81.7577	65.8525	58.9247	312.5783	219.6904	180.0366	150.2405	130.7184	119.6084
	1	107.3134	89.7686	80.3893	70.7582	60.6803	55.8215	231.3419	176.0687	151.6558	132.5523	118.9302	110.5310
	2	79.0425	71.1257	66.4369	61.3051	55.6140	52.6207	166.6481	139.0641	125.9111	115.1420	106.8715	101.3720
	5	60.1668	56.8546	55.0466	53.1436	50.8343	49.4266	119.9581	108.3392	102.9402	98.5989	94.9180	92.2097
	10	52.8268	51.4769	50.7200	49.8508	48.6309	47.8605	99.0056	94.3609	92.3475	90.6808	89.0190	87.7208

For instance, the first dimensionless critical buckling loads of a CC beam with $p_z=1$ and $p_x=1$ are $\bar{N}_{cr1} = 50.0389$ and $\bar{N}_{cr1} = 68.7433$ for $L/h=5$ and $L/h=20$, respectively. On the other hand, the third dimensionless critical buckling loads are $\bar{N}_{cr3} = 102.0339$ and $\bar{N}_{cr1} = 257.1947$ for $L/h=5$ and $L/h=20$, respectively. The relative difference can be obtained by taking the value of the aspect ratio $L/h=5$ as a reference. The relative

difference is % 37 and % 152 for the beams whose aspect ratios are $L/h=5$ and $L/h=20$, respectively. These results can be compared with ones given in [29]. It is clear that the relative difference is the least for CF beam while it is the most for CC beam. And finally, the reduction in the dimensionless critical buckling load because of the gradient index variation in the x direction is more than the gradient index variation in the z direction.

Table 5. The first three dimensionless critical buckling load (\bar{N}_{cr}) of CS two directional FGBs with respect to gradient index and aspect ratio change.

\bar{N}_{cr} P_x	L/h=5						L/h=20						
	P_z						P_z						
	0	0.5	1	2	5	10	0	0.5	1	2	5	10	
\bar{N}_{cr1}	0	89.1357	59.1376	45.7804	35.3019	28.0968	24.9046	108.0501	70.1652	53.9778	42.0824	35.4216	32.1934
	0.5	59.3268	42.6160	35.1359	29.1253	24.6269	22.3796	72.1917	50.8680	41.7999	35.0712	30.8772	28.4093
	1	44.1770	34.2077	29.5659	25.7175	22.6647	20.9894	55.1941	41.6382	35.7437	31.2800	28.2969	26.3745
	2	31.3550	26.5847	24.2979	22.3323	20.5767	19.4609	39.9002	32.8848	29.7709	27.3510	25.5146	24.1789
	5	21.4224	20.0501	19.3880	18.7723	18.0781	17.5929	26.2882	24.3287	23.4544	22.7434	22.0674	21.5191
10	18.2237	17.7798	17.5508	17.3081	16.9948	16.7955	21.8187	21.2520	21.0027	20.7945	20.5745	20.3953	
\bar{N}_{cr2}	0	198.038	134.797	105.174	80.0356	59.7856	51.6226	311.501	202.889	156.216	121.604	101.541	91.9463
	0.5	127.411	94.7184	78.8543	64.7753	52.5819	47.2141	209.103	147.485	121.161	101.444	88.7624	81.4763
	1	89.7116	73.2470	64.5368	56.2745	48.4804	44.6663	158.127	119.829	103.059	90.1574	81.1999	75.5905
	2	64.5511	56.9436	52.7629	48.6012	44.2939	41.9178	113.877	94.4489	85.5772	78.4833	73.0535	69.3370
	5	47.4958	44.8255	43.3788	41.8882	40.1284	39.0177	79.0870	72.4584	69.3673	66.8116	64.5567	62.8214
10	41.4532	40.3655	39.7697	39.1038	38.1927	37.6063	66.0819	63.5965	62.4526	61.4833	60.4897	59.6884	
\bar{N}_{cr3}	0	288.472	200.566	157.589	118.629	84.3219	71.4233	599.307	392.015	302.207	234.735	193.807	174.591
	0.5	176.306	135.164	114.038	93.6128	74.1327	66.0767	401.869	284.607	234.067	195.593	169.756	155.407
	1	122.202	102.060	91.2488	80.1890	68.4781	62.9588	302.110	229.866	198.136	173.282	155.258	144.383
	2	88.8543	79.6596	74.6487	69.3207	63.0290	59.6723	218.475	181.241	164.553	150.876	140.071	132.981
	5	67.5200	64.4788	62.6129	60.4990	57.8659	56.3193	154.830	141.914	135.467	129.946	125.078	121.491
10	59.9997	58.6210	57.8379	56.9168	55.5850	54.7307	131.519	125.314	122.433	119.991	117.559	115.688	

Table 6. The first three dimensionless critical buckling load (\bar{N}_{cr}) of CC two directional FGBs with respect to gradient index and aspect ratio change.

\bar{N}_{cr} P_x	L/h=5						L/h=20						
	P_z						P_z						
	0	0.5	1	2	5	10	0	0.5	1	2	5	10	
\bar{N}_{cr1}	0	152.147	102.270	79.4835	60.8783	46.8870	40.9884	208.951	135.869	104.563	81.4649	68.3268	61.9973
	0.5	99.2471	72.5793	60.1893	49.6843	41.0615	37.0577	137.996	97.6891	80.4917	67.6302	59.4160	54.6228
	1	72.0959	57.3704	50.0389	43.4884	37.7663	34.8959	104.966	79.8051	68.7433	60.2068	54.3477	50.6879
	2	52.0853	44.9833	41.2629	37.7746	34.5080	32.7046	77.3658	63.9889	57.8242	52.8695	49.2052	46.7558
	5	38.8730	35.9533	34.3748	32.8623	31.4285	30.5733	56.6534	51.0839	48.3525	46.0630	44.2740	42.9993
10	34.0348	32.4922	31.6660	30.8925	30.1752	29.6918	49.3614	46.2892	44.7394	43.4082	42.3075	41.4770	
\bar{N}_{cr2}	0	229.951	158.227	123.896	93.7625	68.2770	58.3755	414.574	270.555	208.434	162.090	134.644	121.630
	0.5	144.593	109.331	91.5806	75.1205	60.1253	53.7479	279.274	197.114	161.903	135.367	117.961	108.105
	1	100.027	83.3158	74.1181	64.8638	55.4790	50.9964	209.896	159.439	137.250	120.030	107.804	100.262
	2	72.5250	64.9562	60.5880	55.9515	50.7714	48.0178	150.437	125.215	113.606	104.184	96.8213	91.9228
	5	54.9211	52.0306	50.3343	48.4690	46.2629	45.0337	106.718	97.5788	93.0844	89.2275	86.0168	83.7961
10	48.9775	47.4758	46.5813	45.5963	44.4674	43.8530	93.0553	88.2480	85.7901	83.6473	81.9022	80.6904	
\bar{N}_{cr3}	0	328.380	230.187	181.387	135.983	94.8763	79.8043	777.727	509.989	393.439	305.211	250.356	224.872
	0.5	194.550	151.195	128.661	105.977	83.2961	74.0483	519.575	369.308	304.010	253.740	219.179	200.369
	1	134.706	113.309	102.033	90.2215	76.9552	70.7310	388.804	297.838	257.194	224.692	200.626	186.445
	2	98.3574	88.9166	83.8438	78.1637	71.0194	67.3069	281.920	236.136	214.438	196.131	181.498	172.159
	5	76.7415	73.1927	70.9677	68.4999	65.5587	63.9266	206.971	187.539	177.774	169.447	162.462	157.818
10	68.6959	66.9813	65.9482	64.7539	63.2846	62.4586	177.965	167.285	162.153	157.741	154.084	151.627	

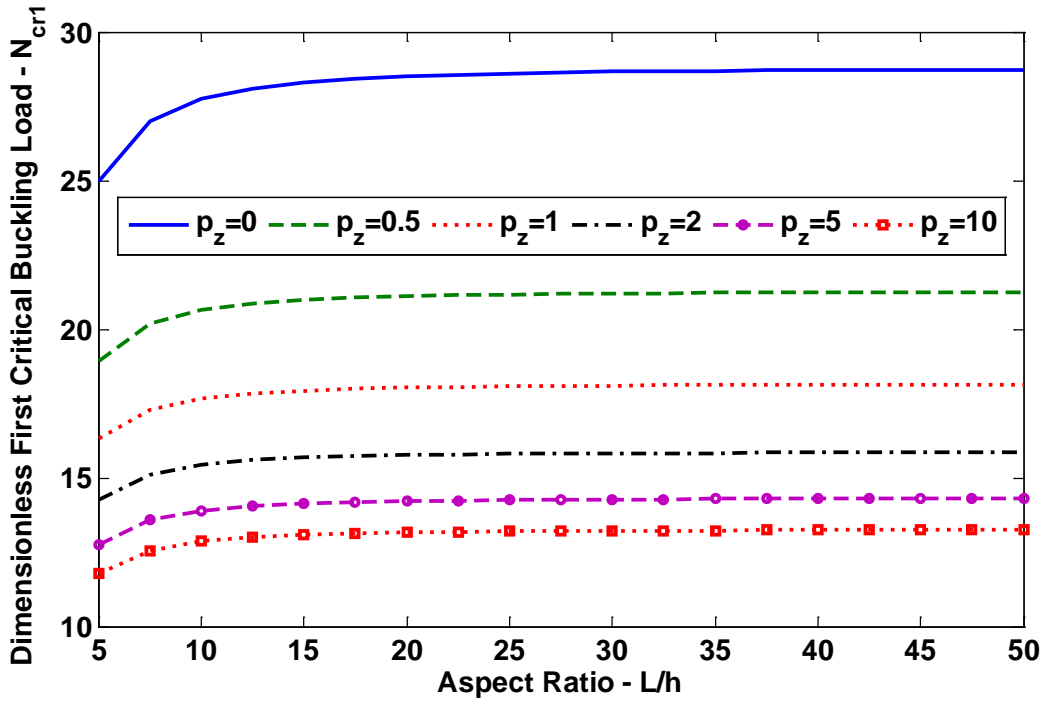
Table 7. The first three dimensionless critical buckling load (\bar{N}_{cr}) of CF two directional FGBs with respect to gradient index and aspect ratio change.

\bar{N}_{cr}	P_x	L/h=5						L/h=20					
		P_z						P_z					
		0	0.5	1	2	5	10	0	0.5	1	2	5	10
\bar{N}_{cr1}	0	13.0595	8.4918	6.5352	5.0916	4.2704	3.8748	13.3730	8.6707	6.6673	5.2021	4.3970	4.0040
	0.5	7.0854	5.2447	4.4705	3.8910	3.4849	3.2202	7.1980	5.3255	4.5425	3.9646	3.5754	3.3129
	1	4.7498	3.9270	3.5691	3.2877	3.0557	2.8893	4.8128	3.9807	3.6222	3.3464	3.1291	2.9658
	2	3.3263	3.0396	2.9107	2.8032	2.6993	2.6209	3.3684	3.0809	2.9542	2.8529	2.7603	2.6856
	5	2.6053	2.5487	2.5223	2.4983	2.4711	2.4516	2.6445	2.5897	2.5659	2.5464	2.5264	2.5098
\bar{N}_{cr2}	0	97.9831	65.0125	50.3292	38.8077	30.8798	27.3685	118.835	77.1690	59.3659	46.2830	38.9569	35.4064
	0.5	63.7453	46.0246	38.1014	31.7083	26.8353	24.3895	77.1676	54.7138	45.1683	38.0747	33.6080	30.9562
	1	47.2172	36.8145	31.9538	27.8875	24.6020	22.8157	58.5561	44.5525	38.4476	33.8066	30.6802	28.6647
	2	33.7261	28.7585	26.3539	24.2643	22.3844	21.2119	42.6719	35.4161	32.1766	29.6492	27.7368	26.3534
	5	23.4348	21.9719	21.2599	20.5936	19.8406	19.3171	28.7449	26.6514	25.7115	24.9455	24.2209	23.6339
\bar{N}_{cr3}	0	204.602	139.275	108.669	82.6915	61.7566	53.3193	321.964	209.705	161.464	125.689	104.951	95.0340
	0.5	131.092	97.5686	81.3034	66.8269	54.1876	48.6291	213.773	151.140	124.379	104.317	91.3612	83.9012
	1	92.1033	75.4135	66.4993	57.9890	49.9087	45.9813	161.416	122.677	105.693	92.6080	83.4999	77.7993
	2	66.4004	58.6117	54.3521	50.0889	45.6390	43.1981	116.622	96.9482	87.9486	80.7438	75.2227	71.4486
	5	49.0431	46.2601	44.7634	43.2237	41.4072	40.2695	81.4278	74.6735	71.5228	68.9152	66.6168	64.8517
	10	42.8001	41.6911	41.0792	40.3924	39.4518	38.8478	68.2404	65.6927	64.5177	63.5212	62.5012	61.6792

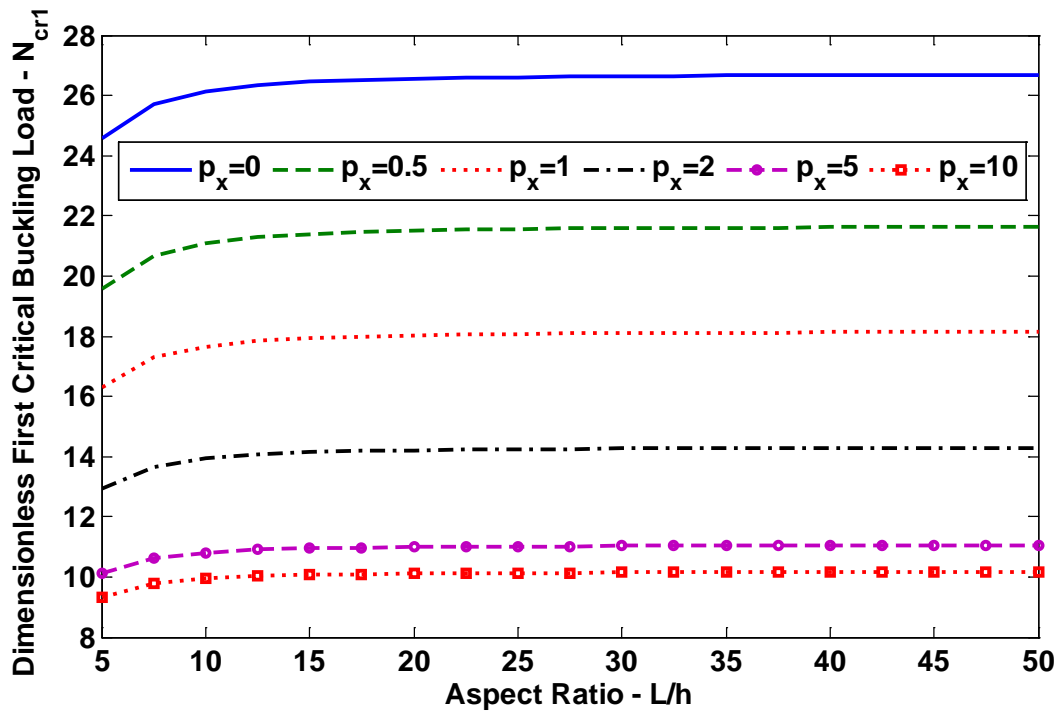
To illustrate the effect of gradient indexes (p_x and p_z) and aspect ratios on the dimensionless buckling loads of the 2D-FGBs for all type of boundary conditions, Figs 2 to 5 are plotted. It is observed that the dimensionless critical buckling load decreases with the increase of the gradient indexes. This is because the rigidity of the beam decreases. Moreover, with the increase of the aspect ratio, the critical buckling loads become very close to each other after in the region of , $L/h \geq 25$ for SS and CS, $L/h \geq 15$ for CF and $L/h \geq 35$ for CC. On the other hand, for CC beams, the effect of the shear deformation is significant in the region of $L/h \leq 15$. It reveals that the effect of the gradient index in

the x direction on the dimensionless critical buckling load is more significant than the gradient index in the z direction for all type of boundary conditions.

The first four normalized buckling mode shapes of the two directional FGBs for all type of boundary conditions are presented in Fig. 6 ($L/h=5$, $p_z=1$ and $p_x=1$). One may expect that for a homogeneous CC beam the mode shapes are symmetric about the midpoint of the beam. However, because of the material variation along the length of the beam the mode shapes become anti-symmetric about the midpoint of the 2D-FGB.

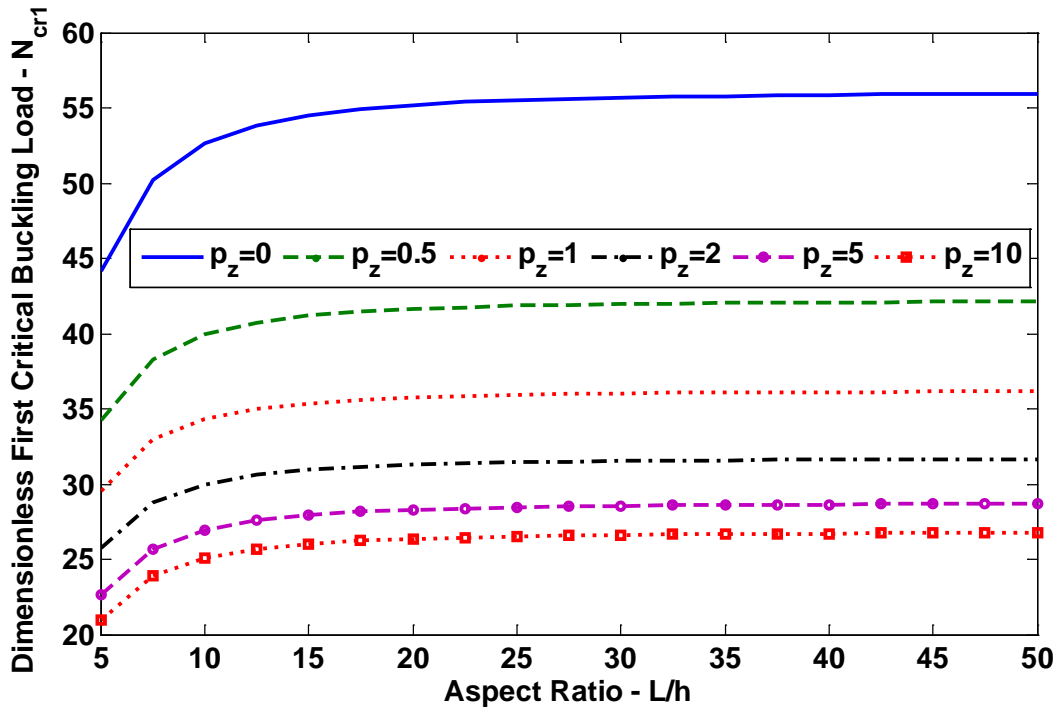


a) $p_x = 1$

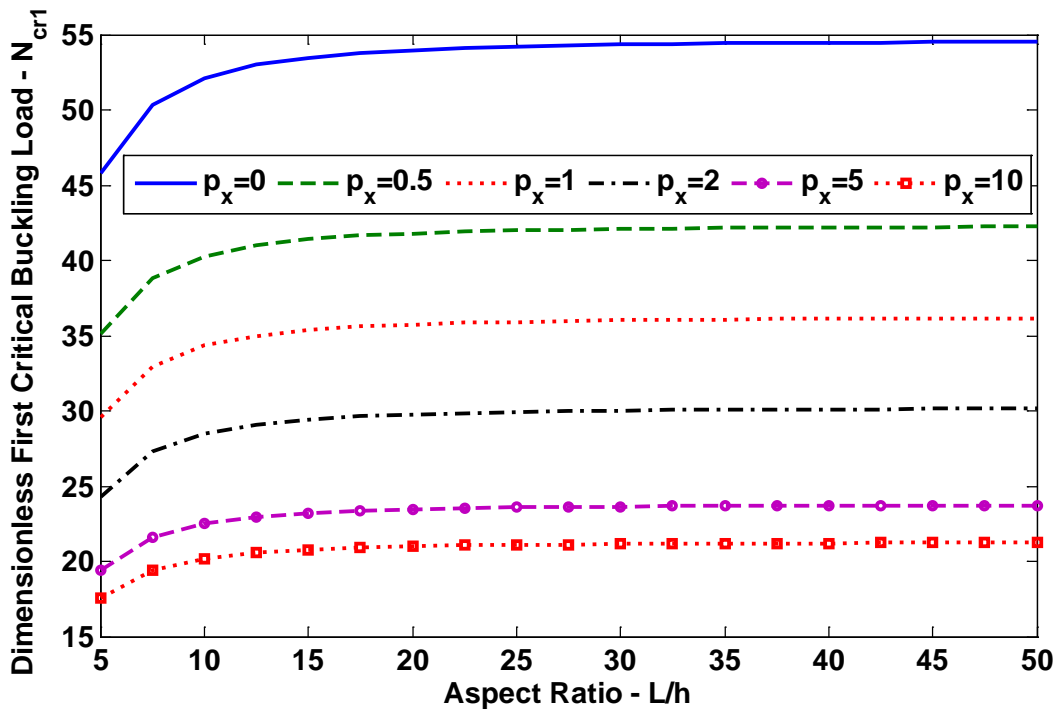


b) $p_z = 1$

Figure 2. Variation of the dimensionless first critical buckling loads of two directional FG SS beams with respect to gradient index a) $p_x = 1$ and b) $p_z = 1$ and various aspect ratios

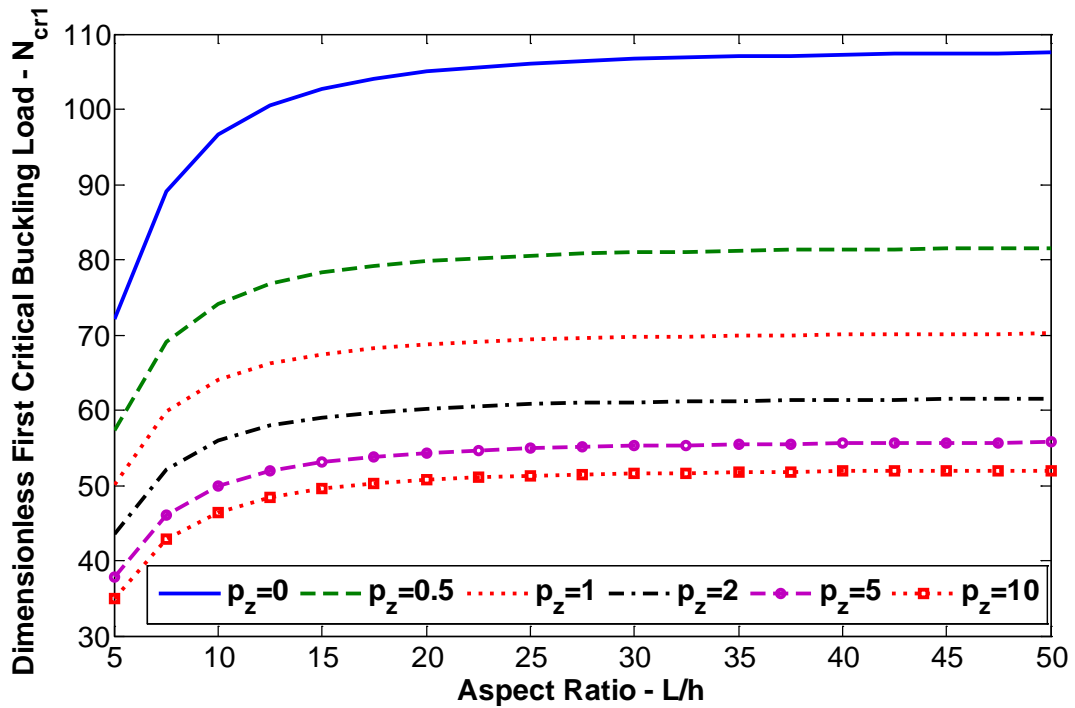


a) $p_x = 1$

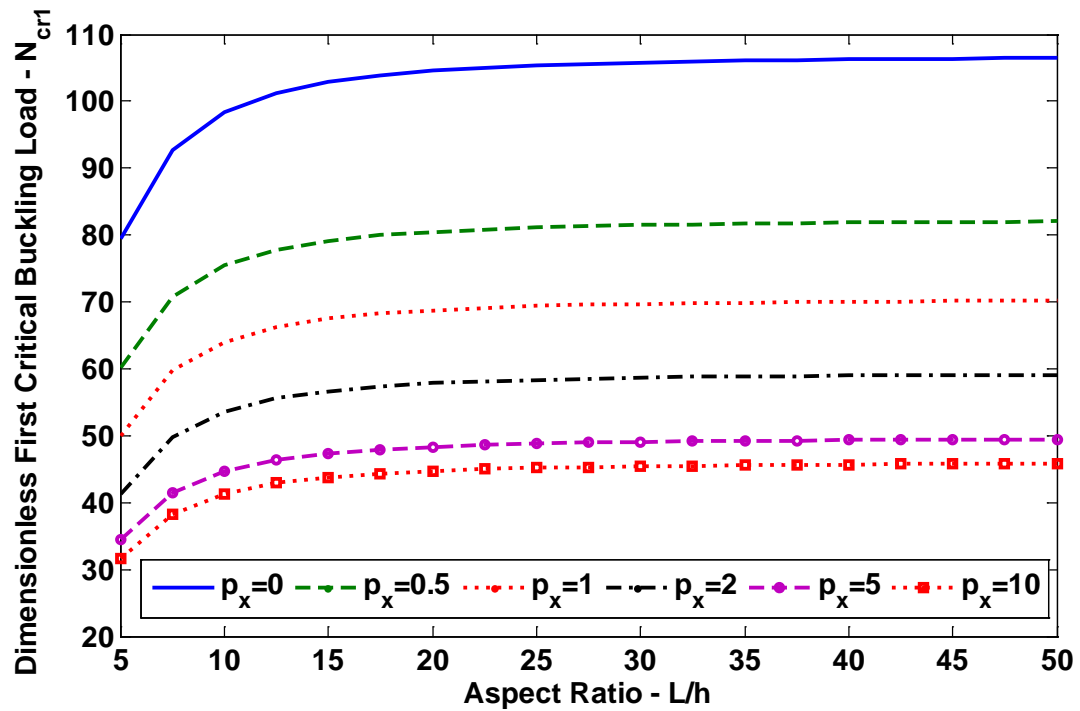


b) $p_z = 1$

Figure 3. Variation of the dimensionless first critical buckling loads of two directional FG CS beams with respect to gradient index a) $p_x = 1$ and b) $p_z = 1$ and various aspect ratios

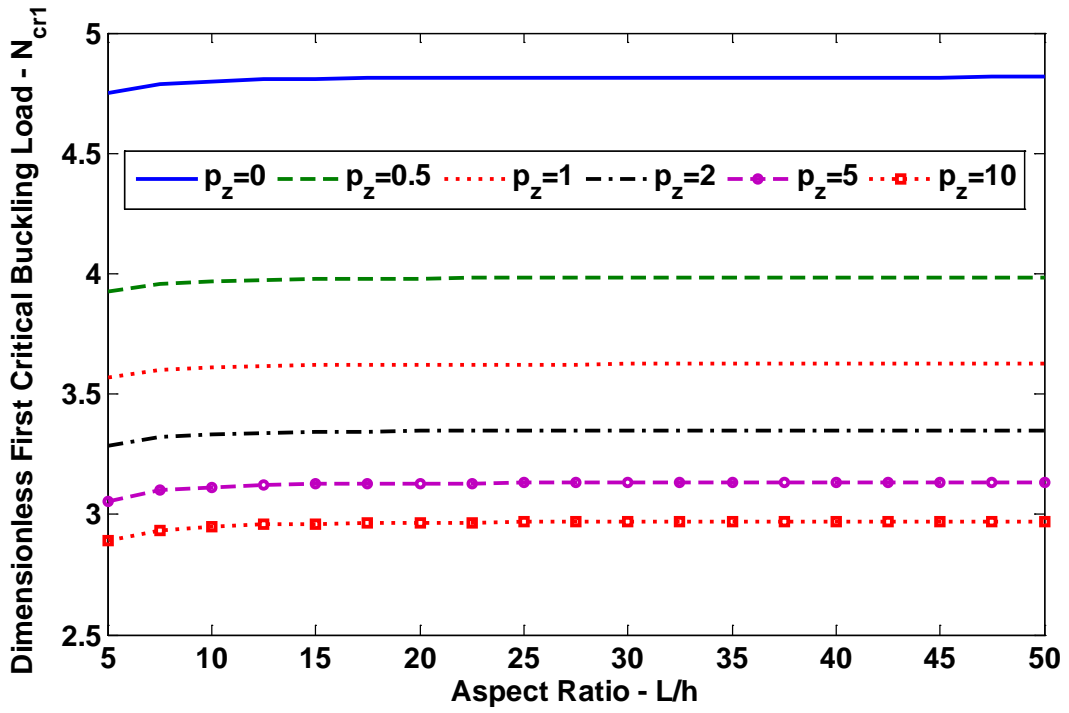


a) $p_x = 1$

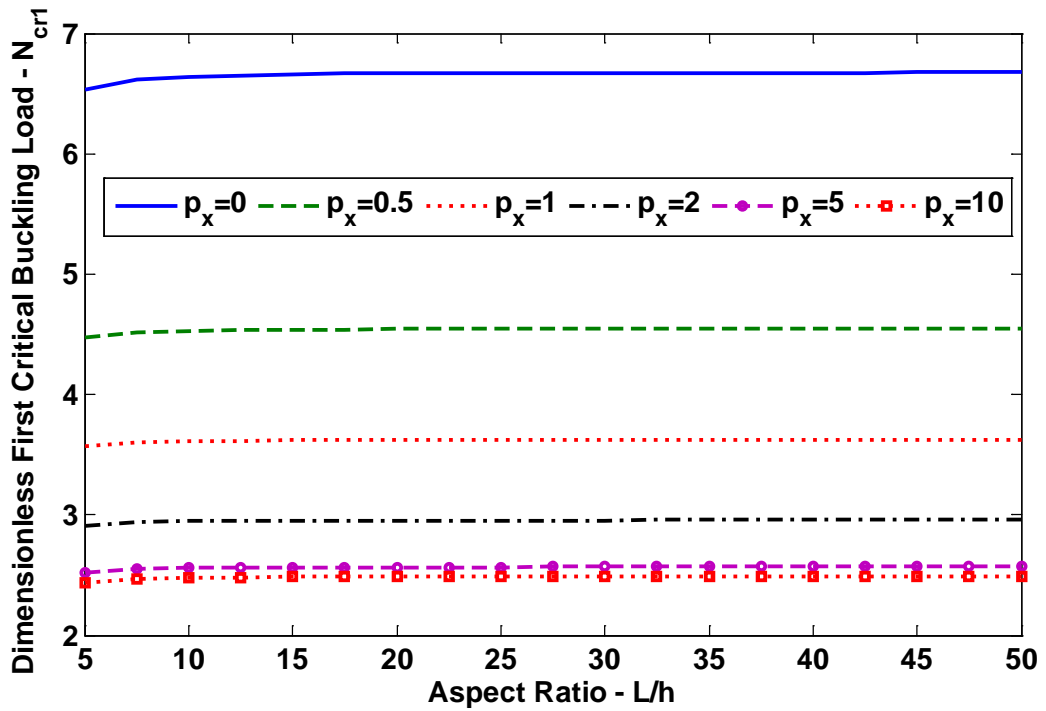


b) $p_z = 1$

Figure 4. Variation of the dimensionless first critical buckling loads of two directional FG CC beams with respect to gradient index a) $p_x = 1$ and b) $p_z = 1$ and various aspect ratios



a) $p_x = 1$



b) $p_z = 1$

Figure 5. Variation of the dimensionless first critical buckling loads of two directional FG CF beams with respect to gradient index a) $p_x = 1$ and b) $p_z = 1$ and various aspect ratios

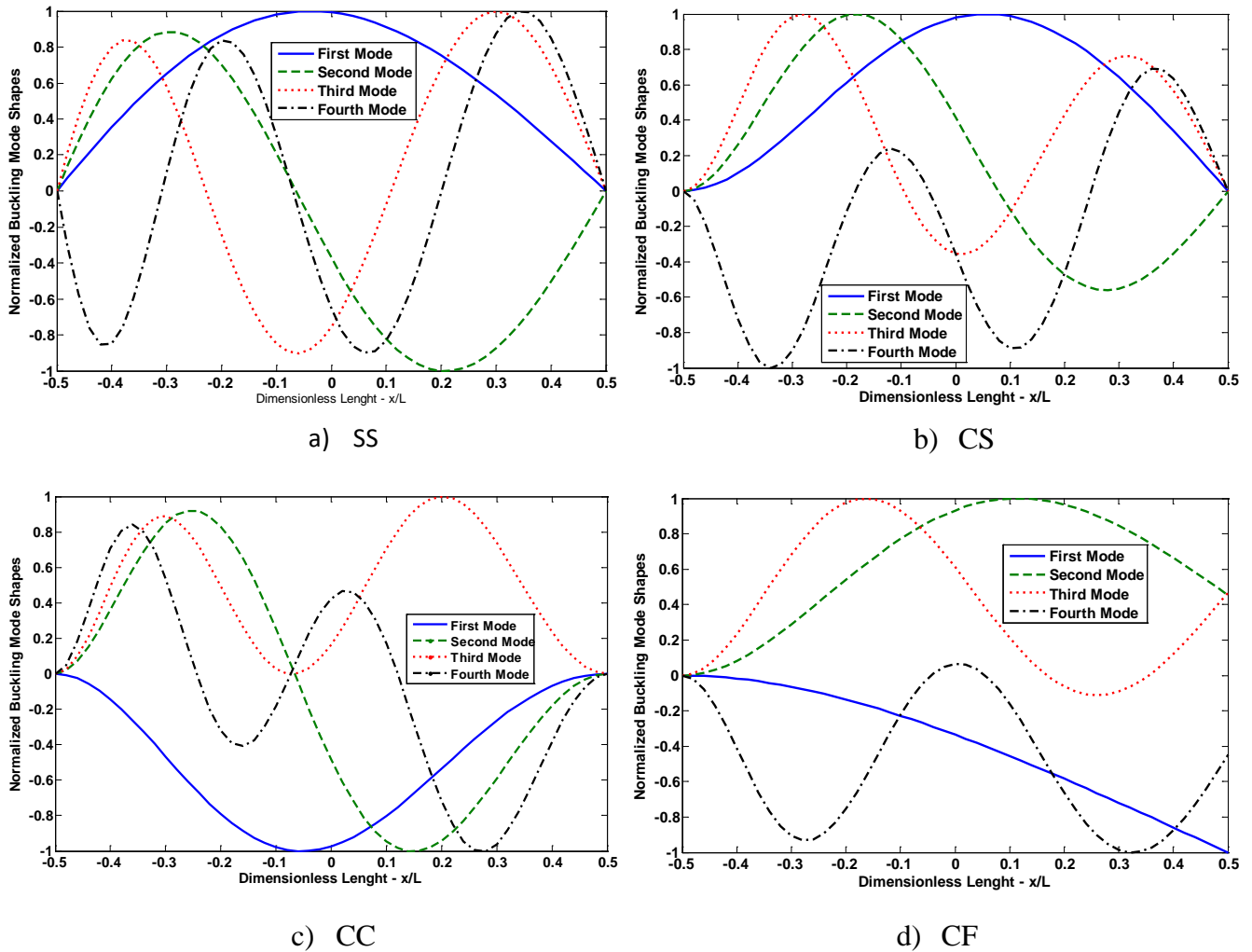


Figure 6. First four normalized buckling mode shapes of the two directional FGBs for various boundary conditions ($L/h=5$, $p_x=1$ and $p_z=1$)

4. CONCLUSION

In this study, the buckling behavior of the two directional functionally graded beams having different boundary conditions is presented. Analytical polynomial series solutions are derived for Simply supported – Simply supported (SS), Clamped-Simply supported (CS), Clamped – clamped (CC) and Clamped-free (CF) boundary conditions by employing various gradient indexes in both axial and thickness directions. The effects of the boundary conditions, gradient indexes and aspect ratios on the critical buckling load of the 2D-FGBs are discussed. By using auxiliary functions the boundary conditions are satisfied. Based on the results obtained by extensive analysis, it is clear that the dimensionless buckling load of the 2D-FGBs is greatly affected by the gradient indexes. However, the effect of the gradient index in the z direction is more significant than the the gradient index in the x direction. To meet the design

requirements, the buckling behavior of the 2D-FGBs can be controlled by selecting suitable gradient indexes. As the aspect ratio increases, the shear deformation effect on the critical buckling loads of the 2D-FGBs decreases. It is observed that CC 2D-FGB is much more sensitive to shear deformation effect than the other 2D-FGB models.

The third order shear deformable beam theory which is employed within this paper for the solution of the buckling behavior of the two directional FGBs satisfies the zero traction boundary conditions on the top and bottom surfaces of the beam, thus a shear correction factor is not required. It allows having a better prediction of buckling response for the 2D-FGBs. Especially for thick beams, the shear deformation effect is very important and higher order shear deformation beam theories are necessary. And finally, the proposed theory provides accurate results and is efficient in solving the buckling behavior of the 2D-FGBs.

REFERENCES

- [1] R. Kadoli, K. Akhtar, N. Ganesan, "Static analysis of functionally graded beams using higher order shear deformation theory", *Appl. Math. Model.*, vol. 32, pp. 2509-2525, 2008.
- [2] X.F. Li, "A unified approach for analyzing static and dynamic behaviors of functionally graded Timoshenko and Euler–Bernoulli beams, *Journal of Sound and Vibration*", vol. 318, pp. 1210-1229, 2008.
- [3] S.R. Li, D.F. Cao, Z.Q. Wan, "Bending solutions of FGM Timoshenko beams from those of the homogenous Euler–Bernoulli beams", *Appl. Math. Model.*, vol. 37, pp. 7077-7085, 2013.
- [4] M. Aydogdu, V. Taskin, "Free vibration analysis of functionally graded beams with simply supported edges", *Materials&Design.*, vol. 28, pp. 1651–1656, 2007.
- [5] M. Simsek, "Fundamental frequency analysis of functionally graded beams by using different higher-order beam theories", *Nuc. Eng. and Des.*, vol. 240, pp. 697–705, 2010.
- [6] M. Simsek, "Vibration analysis of a functionally graded beam under a moving mass by using different beam theories", *Compos. Struct.*, vol. 92, pp. 904–917, 2010.
- [7] K.K. Pradhan, S. Chakraverty, "Free vibration of Euler and Timoshenko functionally graded beams by Rayleigh–Ritz method", *Compos. Part B.*, vol. 51, pp. 175–184, 2013.
- [8] H. Su, J.R. Banerjee, C.W. Cheung, "Dynamic stiffness formulation and free vibration analysis of functionally graded beams", *Compos. Struct.*, vol. 106, pp. 854–862, 2013.
- [9] S.R. Li, Z.G. Wan, J.H. Zhang, "Free vibration of functionally graded beams based on both classical and first-order shear deformation beam theories", *Applied Mathematics and Mechanics*, vol. 35, pp. 591–606, 2014.
- [10] M. Aydogdu, "Semi-inverse method for vibration and buckling of axially functionally graded beams", *Journal of Reinforced Plastics&Composites*, vol. 27, pp. 683–691, 2008.
- [11] Y. Huang, X.F. Li, "Buckling analysis of nonuniform and axially graded columns with varying flexural rigidity", *Journal of Engineering Mechanics*, vol. 137, no.1, pp. 73–81, 2011.
- [12] X.F. Li, B.L. Wang, J.C. Han, "A higher-order theory for static and dynamic analyses of functionally graded beams", *Archive of Applied Mechanics*, vol. 80, pp. 1197-1212, 2010.
- [13] T.P. Vo, H.T. Thai, T.K. Nguyen, F. Inam, J. Lee, "Static behaviour of functionally graded sandwich beams using a quasi-3D theory", *Compos. Part B*, vol. 68, pp. 59-74, 2015.
- [14] M. Filippi, E. Carrera, A.M. Zenkour, "Static analyses of FGM beams by various theories and finite elements", *Compos. Part B*, vol. 72, pp. 1-9, 2015.
- [15] D.S. Mashat, E. Carrera, A.M. Zenkour, S.A.A. Khateeb, M. Filippi, "Free vibration of FGM layered beams by various theories and finite elements", *Compos. Part B*, vol. 59, pp. 269–278, 2014.
- [16] T.P. Vo, H.T. Thai, T.K. Nguyen, F. Inam, J. Lee, "A quasi-3D theory for vibration and buckling of functionally graded sandwich beams", *Compos. Struct.*, vol. 119, pp. 1–12, 2015.
- [17] J.L. Mantari, J. Yarasca, "A simple and accurate generalized shear deformation theory for beams", *Compos. Struct.*, vol. 134, pp. 593–601, 2015.
- [18] J.L. Mantari, "A refined theory with stretching effect for the dynamics analysis of advanced composites on elastic foundation", *Mech. Mater.*, vol. 86, pp. 31–43, 2015.
- [19] J.L. Mantari, "Refined and generalized hybrid type quasi-3D shear deformation theory for the bending analysis of functionally graded shells", *Compos. Part B*, vol. 83, pp. 142–152, 2015.
- [20] T.K. Nguyen, T.P. Vo, B.D. Nguyen, J. Lee, "An analytical solution for buckling and vibration analysis of functionally graded sandwich beams using a quasi-3D shear deformation theory", *Compos. Struct.*, vol. 156, pp. 238-252, 2016.
- [21] T.P. Vo, H.T. Thai, T.K. Nguyen, A. Maheri, J. Lee, "Finite element model for vibration and buckling of functionally graded sandwich beams based on a refined shear deformation theory", *Eng. Struct.*, vol. 64, pp. 12–22, 2014.
- [22] T.K. Nguyen, T.T.P. Nguyen, T.P. Vo, H.T. Thai, "Vibration and buckling analysis of functionally graded sandwich beams by a new higher-order shear deformation theory", *Compos. Part B*, vol. 76, pp. 273–285, 2015.
- [23] M. Nemat-Alla, "Reduction of thermal stresses by developing two-dimensional functionally graded materials", *Int. Journal of Solids and Structures*, vol. 40, pp. 7339–7356, 2003.
- [24] A.J. Goupee, S.S. Vel, "Optimization of natural frequencies of bidirectional functionally graded beams", *Struct. Multidisc. Optim.*, vol. 32, pp. 473–484, 2006.
- [25] C.F. Lü, W.Q. Chen, R.Q. Xu, C.W. Lim, "Semi-analytical elasticity solutions for bidirectional functionally graded beams", *Int. Journal of Solids and Structures*, vol. 45, pp. 258–275, 2008.
- [26] L. Zhao, W.Q. Chen, C.F. Lü, "Symplectic elasticity for two-directional functionally graded materials", *Mech. Mater.*, vol. 54, pp. 32–42, 2012.
- [27] M. Nazargah, "Fully coupled thermo-mechanical analysis of bi-directional FGM beams using NURBS isogeometric finite element approach", *Aerospace Science and Technology*, vol. 45, pp. 154-164, 2015.
- [28] M. Simsek, "Bi-Directional functionally graded materials (BDFGMs) for free and forced vibration of Timoshenko beams with various

boundary conditions”, *Compos. Struct.*, vol. 141, pp. 968–978, 2015.

[29] M. Simsek, “Buckling of Timoshenko beams composed of two-dimensional functionally graded material (2D-FGM) having different boundary conditions”, *Compos. Struct.*, vol. 149 pp. 304–314, 2016.

[30] A. Karamanli, “Elastostatic analysis of two-directional functionally graded beams using various beam theories and Symmetric Smoothed Particle Hydrodynamics method”, *Compos. Struct.*, vol. 160, pp. 653-669, 2017.

[31] A. Pydah, R.C. Batra, “Shear deformation theory using logarithmic function for thick circular beams and analytical solution for bi-directional

functionally graded circular beams”, *Compos. Struct.*, vol. 172, pp. 45-60, 2017.

[32] A. Karamanli, “Bending behaviour of two directional functionally graded sandwich beams by using a quasi-3d shear deformation theory”, *Compos. Struct.*, vol. 174, pp. 70-86, 2017.

[33] T.V. Do, D.K. Nguyen, D.D. Nguyen, D.H. Doan, T.Q. Bui, “Analysis of bi-directional functionally graded plates by FEM and a new third-order shear deformation plate theory”, *Thin-Walled Struct.*, vol. 119, pp. 687-699, 2017.

[34] A. Karamanli, “Free vibration analysis of two directional functionally graded beams using a third order shear deformation theory”, *Compos. Struct.*, vol. 189, pp. 127-136, 2018.